Scale dependence of intragranular porosity, tortuosity, and diffusivity

Robert P. Ewing,[1] Qinhong Hu,[2] and Chongxuan Liu[3]

Received 6 May 2009; revised 13 November 2009; accepted 20 January 2010; published 17 June 2010.

[1] Diffusive exchange of solutes between intragranular pores and flowing water is a recognized but poorly understood contributor to dispersion. Intragranular porosity may also contribute to the "slow sorption" phenomenon. Intragranular pores may be sparsely interconnected, raising the possibility that accessible porosity and diffusive exchange are limited by pore connectivity. We used a pore-scale network model to examine pore connectivity effects on accessible porosity, tortuosity, and diffusivity in spherical particles. The diffusive process simulated was release of a nonsorbing solute initially at equilibrium with the surrounding solution. High-connectivity results were essentially identical to Crank's analytical solution. Low-connectivity results were consistent with observations reported in the literature, with solute released at early times more quickly than indicated by the analytical solution, and more slowly at late times. Values of accessible porosity, tortuosity, and diffusivity scaled with connection probability, distance to the sphere's exterior, and/or the sphere's radius, as predicted by percolation theory. When integrated into a conventional finite difference model, the scaling relationships provide a consistent and physically sound way to incorporate such nonuniformities into models of intragranular diffusion.

Citation: Ewing, R. P., Q. Hu, and C. Liu (2010), Scale dependence of intragranular porosity, tortuosity, and diffusivity, *Water Resour. Res.*, *46*, W06513, doi:10.1029/2009WR008183.

1. Introduction

[2] As water flows through soil, sediment, or rock, solutes may sorb to and desorb from the solid material. This sorption/desorption process can be a major contributor to dispersion of the solute: A sorbing solute may persist in a sorbed state long after its upgradient aqueous concentration has dropped to a negligible value. Sorbed solute may then desorb over a long time, giving persistent nonnegligible concentrations downgradient. When the solute is toxic even at extremely low concentrations, this "long tailing" can greatly increase the necessity, difficulty, and expense of remediation.

[3] A peculiarity of sorption/desorption behavior, first noticed with hydrophobic organic compounds in geological porous media [*Steinberg et al.*, 1987], is the so-called slow sorption (or aging) phenomenon. In slow sorption, longer exposure of the medium to the solute results in lower desorption rates [*Hatzinger and Alexander*, 1995], and/or to a greater fraction appearing to be irreversibly sorbed [*Ten Hulscher et al.*, 2005]. Subsurface contaminants may be in the ground for years or decades before they are discovered and targeted for remediation [e.g., *Eberhardt and Grathwohl*, 2002], allowing contaminants to migrate into slow diffusion domains. Contaminants in these slow domains will then diffuse back to more mobile regions during and after aquifer remediation, with this back-diffusion potentially requiring decades [*Steinberg et al.*, 1987; *Eberhardt and Grathwohl*, 2002]. The process need not be purely diffusive: If the sorption isotherm is linear or nearly linear [*Young and Ball*, 1994] within the range of concentrations observed, then diffusion with sorption is indistinguishable from diffusion without; only the apparent diffusion rate is different [*Crank*, 1975].

[4] Early studies of the role of sorption in solute dispersion assumed that sorption equilibrium was reached instantly [*Valocchi*, 1985], but it is now recognized that this is rarely the case. Two classes of conceptual models have been proposed to describe this nonequilibrium. One model, sorption (or chemical) nonequilibrium, posits the existence of more than one kind of sorption site: perhaps two (one instantaneous, the other time-dependent [e.g., *Weber et al.*, 1998]), or perhaps several. The other model, transport (or physical) nonequilibrium, posits that diffusion to sorption sites is the rate-limiting step, with solutes diffusing between regions of flowing and stagnant water, and/or within mineral and/or organic components of the medium [*Wu and Gschwend*, 1986; *Wood et al.*, 1990; *Pignatello and Xing*, 1996]. Combinations of these two models (multiprocess nonequilibrium models [*Brusseau et al.*, 1989, 1992]) have also been developed. Realistically, both sorption and transport nonequilibrium probably occur in most soils and aquifers, with one or the other being rate-limiting depending on specifics of the situation [*Crank*, 1975; *Ho et al.*, 2000]. While the two conceptual models are mathematically equivalent when sorption/desorption reactions follow a linear

[1]Department of Agronomy, Iowa State University, Ames, Iowa, USA.
[2]Department of Earth and Environmental Sciences, University of Texas at Arlington, Arlington, Texas, USA.
[3]Chemical and Material Science Division, Fundamental and Computational Science Directorate, Pacific Northwest National Laboratory, Richland, Washington, USA.

0043-1397/10/2009WR008183

isotherm [*Nkedi-Kizza et al.*, 1985; *Haggerty and Gorelick*, 1995], the mechanisms, and therefore the implications for remediation, are quite different. Understanding the slow sorption process therefore has utility in assessing future risks under various remediation and monitoring scenarios.

[5] This study focuses on the transport nonequilibrium (diffusion-mediated) model, of which many refinements have been proposed. Expanding the model to account for different particle sizes [*Cunningham and Roberts*, 1998] and mineralogies [*Kleineidam et al.*, 1999; *Liedl and Ptak*, 2003] has proven useful. A branched pore model [e.g., *Ko et al.*, 2003] has been used to good effect with charcoal and similar materials, but only rarely in mineral-based materials [e.g., *Werth and Reinhard*, 1997]. The branched pore model characterizes intragranular porosity as being composed of both mesopores and micropores: The mesopores have faster diffusion, while the micropores have more sorption sites. Other hierarchical pore arrangements have also been proposed [e.g., *Arocha et al.*, 1996; *Cunningham et al.*, 1997], as well as models imposing unrealistic restrictions on pore topology [e.g., *Haggerty and Gorelick*, 1998]. Observed increases in the apparent diffusion coefficient $\mathcal{D}_{app}$ in the presence of a cosolvent [*Li and Werth*, 2004], and sharpening of the diffusion front during sorption in contrast to spreading of the front during desorption, have raised the possibility of concentration-dependent diffusion. But because apparent concentration-dependent behavior can also be caused by nonlinear isotherms [*Nestle and Kimmich*, 1996], which are ubiquitous in soils, it is not necessary to invoke concentration-dependent diffusion to explain the observations.

[6] Despite these and other refinements, diffusion-based models frequently predict too little early desorption, and/or too much late desorption, to match the data. Examples of this pattern include *Pedit and Miller* [1994, Figures 2 and 4], *Harmon and Roberts* [1994, Figures 5 and 6], *Cornelissen et al.* [1997, Figures 1 and 2], *Fleming and Haggerty* [2001, Figure 6], *Werth and Hansen* [2002, Figures 1–4], and *Niedermeier and Loehr* [2005, Figures 3–5]. This "too-long tailing" may be partially explained by recognizing that soil solids are not actually spherical: For a given volume, nonspherical particles have more surface area, and more of their interior is close to the edge [*Heyse et al.*, 1999; *Başağaoğlu et al.*, 2002]. More recently, *Başağaoğlu et al.* [2004] conjectured that intragranular pores near the grain's surface are both larger, and more numerous, than pores deeper inside. Implementing these modifications in a radial diffusion model yielded the desired increased tailing; unfortunately, no evidence or rigorous justification was provided for them.

[7] This study proposes that intragranular porosity is frequently nonuniform and should give results similar to those seen by *Başağaoğlu et al.* [2004]. However, the range and extent of effects of this nonuniform porosity are likely greater than they implied. We use percolation theory and pore-scale network modeling to examine a specific cause of nonuniform porosity, to assess its effects on intragranular diffusion, and to show how the resulting diffusion may present as slow sorption.

2. Background

[8] Most rocks and soil solids have quite low internal porosity, but many are permeable nonetheless. The conductivity of a saturated rock, whether hydraulic or electrical, decreases as porosity decreases. *Archie* [1942] first formalized a relationship between porosity and electrical conductivity, given in its simplest form as $\sigma/\sigma_0 \sim \phi^m$ (where σ is electrical conductivity of brine-saturated rock, σ_0 is the conductivity of the brine, ϕ is porosity, and the exponent m is often around 2). This power law relationship can be derived [*Hunt*, 2004] by assuming that as the porosity decreases, the density of pore connections also decreases. As pore connectivity decreases, the density of conducting pathways also decreases while their tortuosity increases; the net result is a strong decrease in conductivity. This conceptual model can be extended to include surface conduction [*Ewing and Hunt*, 2006].

[9] Percolation theory, the study of pathways in disordered media [*Stauffer and Aharony*, 1994], makes predictions that can be readily tested in material such as rock matrices [*Hunt and Ewing*, 2009]. For example, just above the percolation threshold (the connection density at which a continuous pathway across the medium is established) the electrical conductivity is expected to scale as $\sigma(\theta) \sim (\theta - \theta_c)^{\mu}$, where θ is the volume fraction of the conducting phase, θ_c is its critical value (often around 0.1ϕ in soils), and the exponent $\mu = 2.0$. This Archie-like relationship holds, for example, for electrical conductivity in unsaturated media [*Ewing and Hunt*, 2006], and for hydraulic conductivity at low water contents [*Hunt*, 2005].

[10] The (total) porosity ϕ of a porous material is the sum of its accessible porosity ϕ_a and its isolated porosity ϕ_i. Most measurement methods give the accessible porosity, which is assumed to be distributed uniformly within the medium. However, when the pore connectivity is low, the probability of finding a continuous pathway from the exterior to some interior point decreases with increasing distance of that point from the exterior. This results in accessible porosity decreasing with increasing distance from the exterior surface, generally reaching a stable value after some characteristic distance. For example, tracer concentrations have been observed to decrease with increasing distance from the rock face [*Hu et al.*, 2006; *Cvetkovic and Cheng*, 2008; *Xu and Wörman*, 1999] despite tracer equilibrium having been attained; the observed concentration profiles are consistent with percolation theory.

[11] Percolation theory also predicts that just above the percolation threshold, a diffusion-like process proceeding from an inlet face will display two distinct behaviors. For example, imbibition (mathematically a diffusive process) into dry low-connectivity rock may show cumulative "infiltration" scaling with time as $I \sim t^{0.26}$ at early times [*Hu and Ewing*, 2002; *Hu et al.*, 2006], reverting at later times to the classical $I \sim t^{0.5}$ [*Philip*, 1957]. Simulations of diffusion in low-connectivity media show exactly this behavior [*Ewing and Horton*, 2002; *Ewing*, 2009]. The distance from the imbibition face at which the behavior changes scales with the correlation length χ of percolation theory, given by

$$\chi = a|p - p_c|^{-\nu}, \tag{1}$$

where p represents the probability of a site, bond, or pore (as appropriate) being active, p_c is its critical value, the exponent $\nu \approx 0.88$ in three dimensions, and the prefactor a is based on specifics of the system being examined. As the percolation threshold is approached, χ goes to infinity.

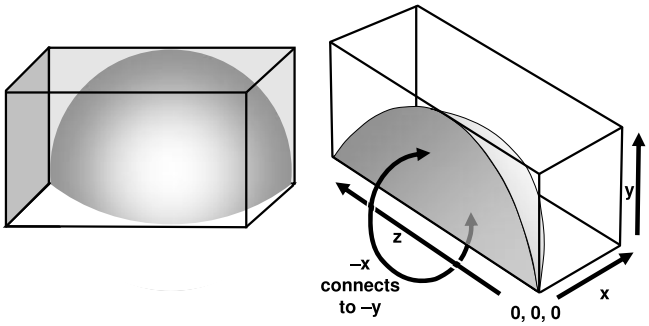

Figure 1. Diagram of the quarter-sphere configuration used in the modeling.

[12] Rock-forming processes in nature frequently produce both fracture networks and rock matrices with connectivities just above the percolation threshold. Rocks are subject to stresses which fracture them over a wide range of scales. Formation of a continuous crack network, one just above the percolation threshold, relieves some of the stress, potentially halting the cracking [*Chelidze*, 1982; *Gueguen et al.*, 1997]. A similar process appears to take place in cooling magma [*Cheadle et al.*, 2004; *Price et al.*, 2006]: As crystals grow outward toward each other, the remaining melt is pushed out through interstitial pores. At the end of the process the grain boundaries do not match perfectly, leaving grain boundary networks that are well described by percolation theory [*Zhu and Hirth*, 2003; *Frary and Schuh*, 2005]. An analogous argument applies to diagenetic cementation of sedimentary rock [*Karmakar et al.*, 2003]: As (for example) carbonate is deposited, porosity and permeability decrease. Eventually the rate at which more carbonate can be transported in approaches zero.

[13] Percolation theory is typically used to estimate bulk properties (e.g., diffusivity) in settings where edge effects are not important. Our use of it here for individual spheres, with near-surface variations in properties dominating the bulk behavior, is a novel application.

3. Methods

[14] Pore-scale network models are useful tools for examining implications of low pore connectivity, especially when used to complement careful laboratory measurements [e.g., *Hu et al.*, 2006]. A pore-scale network model was developed to examine porosity, tortuosity, and diffusivity within spherical particles as a function of their size and pore connectivity. The basics of the model and its validation are described by *Ewing and Horton* [2002]. In essence, the model consists of a simple cubic lattice of sites connected by bonds, with the probability p of active bonds specified by the user, and the selection of which specific bonds are active determined randomly. Active bonds represent working connections; inactive bonds may be thought of as nonexistent. In the simple cubic lattice, the bond percolation threshold p_c is reached when bonds are active with a connection probability $p = 0.2488$. Simulations were run using multiple connection probabilities in $0.24 \leq p \leq 1.0$. The specific implementation for this study used a cubic lattice measuring $L(x) \times L(y) \times 2L(z)$ sites, where L takes values of 11, 21, 51, 101, 201, 501, and 1001 lattice units. Within this "box," those sites no more than a distance $R \equiv L - 1$ from the point (1, 1, L) are considered to be inside a solid sphere (Figure 1), and have pore connection probability p. Sites outside the sphere have connectivity $p = 1.0$. The 1:1:2 proportion allows for periodic boundary conditions in two dimensions: A site in the sphere located at $(1, y, z)$ which has an active bond in the $-x$ direction is connected to the site at $(y, 1, z)$ via the $-y$ direction. It was not clear how to connect three cut faces (e.g., 1/8 of a sphere, with the center in one corner of a cube); having periodic boundaries that connect just two faces was simpler, so simulations used a quarter sphere (Figure 1).

[15] The sites (bond intersections) in this model represent the intragranular pores, and all intragranular porosity is attributed to them. Each individual pore body is entirely characterized by its (x, y, z) location and by which of its six bonds are active. Pore bodies and throats are not assigned a radius, wall roughness, sorption capacity, tortuosity, or any other property. Macroscopic system properties emerge based solely on the connection probability p and (in some cases) the sphere radius R. While our model uses a simple cubic lattice, the universality property of percolation theory [*Stauffer and Aharony*, 1994] allows us to apply the resulting scaling relationships more generally. For example, an equation such as (1) may have a prefactor (proportionality constant) that is specific to our cubic lattice, but the value of the exponent ν (0.88 in three dimensions) applies to different lattices, including irregular topologies.

[16] Two suites of numerical investigations were pursued. In the first, the accessible porosity ϕ_a and distance from each pore to the exterior were examined as functions of sphere size and connectivity. We distinguish between total and accessible (i.e., connected to the sphere's exterior) porosity, because isolated (inaccessible) pores play no role in solute transport. The first suite of investigations therefore consists of mapping sphere interiors to determine which pores are accessible. In this mapping, two parameters are calculated and recorded for each accessible pore: the pore's straight-line or Euclidean shortest distance to the sphere's exterior, herein denoted l, and the length of the shortest pathway connecting it to the sphere's exterior, herein denoted λ. This second value is called "chemical distance" in the percolation literature, because it represents the shortest pathway a diffusing chemical can take between two given points.

[17] In the second suite of numerical experiments, tracers in the form of random walkers were randomly emplaced into accessible pores and made to diffuse out. Diffusion consists of repeatedly choosing a direction (positive or negative x, y, or z) at random and, if the bond in that direction is active, moving the random walker to the corresponding nearest-neighbor site. Each tracer is moved until it exits the sphere; at that moment it is considered to have desorbed, and the number of elapsed time steps is recorded. The simulation is therefore exactly analogous to an experiment that starts with porous spheres at 100% equilibrium with a tracer solution; the bulk solution's concentration is then changed to and maintained at zero, and tracer release proceeds until none remains in the spheres. The differences lie mainly in the abstraction of pore geometry and time scale, and the absence of sorption. As with the first suite of experiments, the main independent variables are the sphere's size and the pore connectivity.

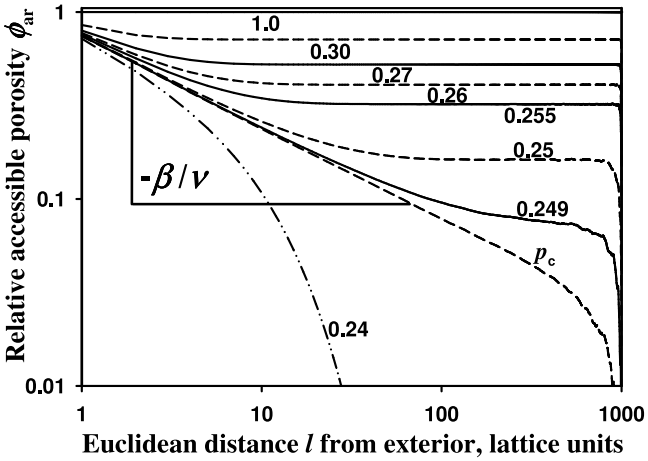

Figure 2. Relative accessible porosity ϕ_{ar} as a function of Euclidean distance l from the exterior of a sphere with radius $R = 1000$ lattice units. The diagonal line for $p = p_c$ is given by equation (4).

[18] Monte Carlo simulations were run with 100 realizations, with each realization differing from the others solely in the random number seed used. Each diffusion simulation used 10,000 random walkers per realization. The Mersenne Twister [*Matsumoto and Nishimura*, 1998] was used to generate the pseudorandom numbers. A quarter sphere of radius $R = 1000$ occupied approximately 2 GB of RAM and at the percolation threshold required about 8 min to map on a dedicated 3.4 GHz Pentium 4. On the same computer, simulating desorption of just 250 random walkers from a sphere with $R = 500$ and $p = p_c$ required several weeks, so no desorption simulations were run on spheres of $R = 1000$, or for $R = 500$ and $p_c \le p < 0.25$.

4. Results

4.1. Accessible Porosity Distribution

[19] Because simulations were conducted using a simple cubic lattice, the simulated porosity distribution as a function of distance from the sphere's exterior is not precisely that given by geometrical analysis. At complete connectivity ($p = 1.0$), at a distance l from the sphere's exterior, and comparing spherical shells that are one lattice unit in thickness, the ratio of cubic lattice and analytical geometry accessible volumes is empirically given as

$$\frac{\text{cubic lattice } V_a(l)}{\text{analytical } V_a(l)} \approx \frac{5}{6} + \left(\frac{l}{R}\right)^{1.5}, \tag{2}$$

where accessible volume V_a for the cubic lattice is given as the number of accessible sites. To avoid the distraction of this distinction, simulated accessible porosity at a given connection probability p and distance l will be given relative to the corresponding simulated V_a at $p = 1.0$,

$$\phi_{ar}(p,l) \equiv \frac{V_a(p,l)}{V_a(p=1.0,l)}, \tag{3}$$

with the subscript r signifying that the accessible porosity is relative. In other words, porosity results are not "converted" to the analytical geometry values, but are simply normalized with respect to a fully connected cubic lattice.

[20] The relative accessible porosity ϕ_{ar} decreases as the connection probability is decreased from $p = 1.0$ to the percolation threshold (Figure 2). In particular, the relative accessible porosity changes from being uniformly distributed with l at $p = 1.0$, to decreasing rapidly with increasing l at connection probabilities close to p_c. At the percolation threshold, relative accessible porosity at a distance l from the sphere's exterior is given by

$$\phi_{ar}(p_c,l) = \phi_0 l^{-\beta/\nu}, \tag{4}$$

where the exponent β ($\approx$0.41 in three dimensions) relates to the "power" (size or density) of the infinite cluster. Finite size issues tend to alter scaling by a factor of the distance raised to the $1/\nu$ power, so the power $-\beta/\nu$ is expected for finite size spheres. The prefactor ϕ_0 is the accessible porosity at $l = 1$, empirically taking the value $\phi_0 = 0.744$ at $p = p_c$. More generally (and again empirically),

$$\phi_0 = \min[1, 0.744 + b(p - p_c)], \tag{5}$$

where b is discussed below.

[21] For $p > p_c$, the correlation length χ is finite, and at distances from the surface greater than the correlation length but less than the radius ($R > l > \chi$), the relative accessible porosity reaches a stable value which cannot exceed 1.0. For $p > p_c$ the stable value (Figure 2) is

$$\phi_{ar}(p,l) = \min\left[1, b(p - p_c)^{\beta}\right]. \tag{6}$$

The two lines (equations (4) and (6)) intersect at the correlation length $\chi \equiv a\,(p - p_c)^{-\nu}$ (equation (1)), giving us an expression for b:

$$b = \frac{\phi_0 [a(p - p_c)^{-\nu}]^{-\beta/\nu}}{(p - p_c)^{\beta}}. \tag{7}$$

Fitting (4) and (6) to the simulation results across all values of p and l gives $a \approx 0.07$, after which values for ϕ_0 and b can be obtained iteratively via (5) and (7). Equations (4) and (6) can be multiplied by the total pore volume of the "layer" or shell at a distance l from the sphere's exterior; summing over all values of l gives the total accessible volume V_a. For the values of p and R examined, V_a spanned more than 6 orders of magnitude, and all estimates were within a few percent of the simulated values.

4.2. Chemical Distance and Tortuosity

[22] Using a pore-scale network model, it is straightforward to calculate the mean chemical distance λ of pores at a given Euclidean distance from the sphere's exterior. In contrast to the Euclidean distance l discussed above, the chemical distance from the exterior to pores near the sphere's center can be greater than the sphere's radius. Chemical distance increases as a superlinear function of l as p approaches p_c (Figure 3a): For distances less than the correlation length we see $\lambda(l) \sim l^{D\min}$. The exponent $D_{\min}$ ($\approx$1.34 in three dimensions) is interpreted as the fractal dimension of the shortest (minimal) path between any two

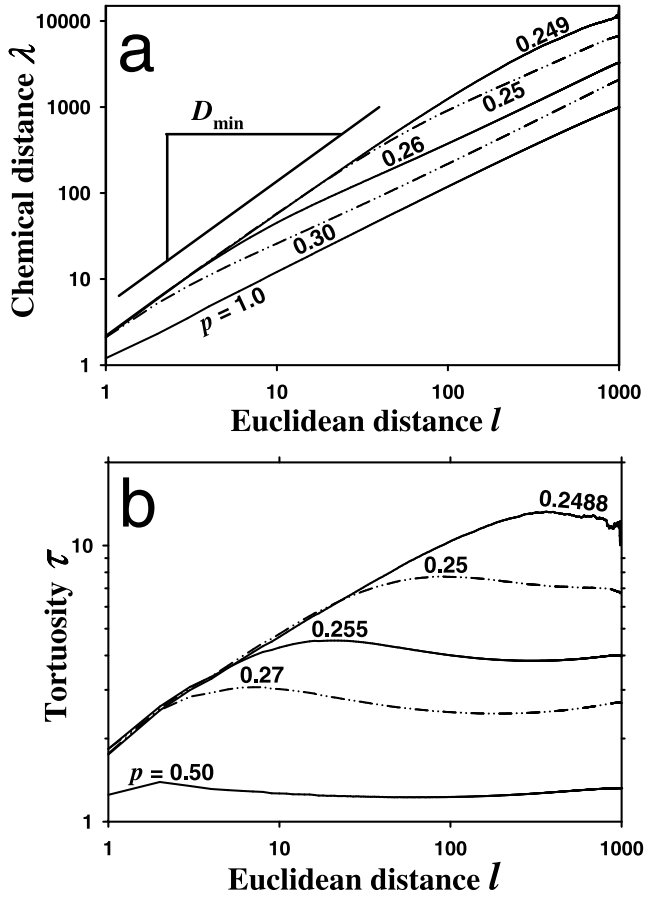

Figure 3. (a) Chemical distance λ as a function of Euclidean distance l from the exterior of a sphere with $R = 1000$, at several connection probabilities p. (b) Tortuosity τ ($\equiv \lambda/l$) as a function of Euclidean distance l from the exterior of a sphere with $R = 1000$. Numbers are normalized with respect to the $p = 1.0$ tortuosity, which due to cubic lattice artifacts is slightly greater than 1.0.

connected points [*Stauffer and Aharony*, 1994]. One expects $\lambda(l)$ to be linear for distances $l > \chi$, giving

$$\lambda(l,p) = \tau_0 \begin{cases} l^{D_{\min}} & l < \chi \\ (l-\chi) + \chi^{D_{\min}} & l > \chi \end{cases}. \quad (8)$$

The prefactor τ_0 for the cubic lattice was found empirically to be approximately

$$\tau_0 = \min[2.2, 1.077 - 0.7785 \log(p - p_c)]. \quad (9)$$

Simulation results indicate that the correlation length with respect to chemical distance is approximately 3 times greater than that with respect to accessible porosity. But there can be only one correlation length, so we interpret this as meaning that this apparent correlation length for chemical distance is 3 times the real correlation distance χ. Equation (8) should therefore, for our specific geometry, have all instances of "χ" replaced by "3χ."

[23] Taking the ratio $\tau(l) \equiv \lambda(l)/l$ yields what is generally called tortuosity τ:

$$\tau(l,p) = \tau_0 \begin{cases} l^{D_{\min}-1} & l < 3\chi \\ (3\chi)^{D_{\min}-1} & l > 3\chi \end{cases}. \quad (10)$$

After normalizing with respect to $\tau(l)$ for $p = 1.0$ to reduce artifacts due to using a cubic lattice, we get results that are a good match to the expected behavior (Figure 3b). Because the infinite cluster is essentially homogeneous at scales greater than χ [*Stauffer and Aharony*, 1994], we expect τ to be constant beyond χ (or 3χ in this specific case). The slight decrease seen at $l > 3\chi$, especially close to the sphere's center, is an artifact of the spherical particles: The longest pathways compete for a rapidly diminishing volume near the center. We do not see this decrease in nonspherical geometries (R. P. Ewing and A. G. Hunt, unpublished data, 2007).

[24] Recall *Başağaoğlu et al.*'s [2004] conjecture that a nonuniform distribution of porosity with distance into the sphere may be the cause of the observed faster-than-expected early time release of solutes, followed by a slower-than-expected late-time release. Here we clarify that the disparity between observed and classical (analytical) desorption curves may be caused by the nonuniform distribution of accessible porosity with chemical distance: Only accessible porosity is involved, and it is chemical distance (λ), rather than the Euclidean distance (l), that is relevant to the diffusion process. To our knowledge, no previous studies have examined the relationship between chemical and Euclidean distance in spheres near the percolation threshold.

[25] While the ratio λ/l is often simply denoted tortuosity τ (sometimes further specified as geometrical tortuosity [*Clennell*, 1997]), the concept is not so simple. Theoretically, tortuosity decreases a system's conductivity or diffusivity by a factor τ^{-2}. The square is required because both the distance traveled, and the distance over which the gradient applies, are increased by the tortuosity [e.g., *Scheidegger*, 1960; *Bear*, 1972; *Dykhuizen and Casey*, 1989; *Epstein*, 1989; *Moldrup et al.*, 2001]. But when relating tortuosity to time rather than to effective diffusivity, the effect of tortuosity must be squared again, because in diffusive processes the mean passage time scales with the square of the (chemical) path length. This means that for a given sphere size R, the expected time for release of the last solutes increases with tortuosity as

$$\frac{t(\tau > 1)}{t(\tau = 1)} \sim \tau^4 \equiv \left(\frac{\lambda}{l}\right)^4. \quad (11)$$

For example, a tortuosity value $\lambda/l = 10$ increases the solute release time by a factor of 10,000. If either square were omitted, this increase in time could be (erroneously) interpreted as $\tau = 100$; if both were omitted, as $\tau = 10{,}000$. Because such values are hard to defend geometrically [*Scott*, 2001], tortuosity is often treated as a fitting parameter without physical meaning [e.g., *Dykhuizen and Casey*, 1989; *Ball and Roberts*, 1991]. But a physical theory should make physical sense. We suspect that the geometrically indefensible tortuosities occasionally obtained as fit-

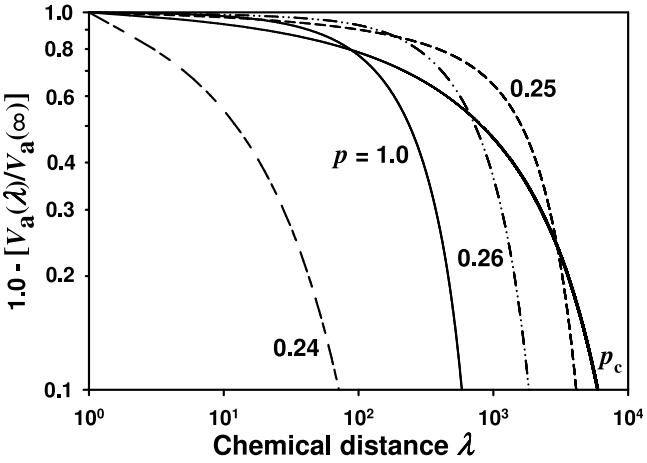

Figure 4. Fraction of the total accessible volume that is within a chemical distance λ from the exterior, $V_a(\lambda)/V_a(\infty)$, in a sphere with $R = 1000$.

ting parameters often result from a failure to account for (1) tortuosity decreasing transport by its inverse squared, and/or (2) mean passage time increasing with chemical distance squared in diffusive processes.

[26] An inconvenient consequence of equation (8) and/or (10) is that except for simple cases such as steady state one-dimensional through-diffusion, a single tortuosity value is inadequate to properly characterize a low-connectivity medium. Rather, the tortuosity is a function of both the Euclidean distance from the surface, and the proximity of the pore space to the percolation threshold. The fractal nature of tortuosity for $l < \chi$ defies the use of a simple ratio. We can, however, put an upper bound on the maximum chemical distance: At $p = p_c$ the correlation length is infinite, so a porous sphere at the percolation threshold can be expected to have its most chemically distant pore at $\lambda_{max} \sim R^{D_{min}}$.

[27] It is instructive to examine the distribution of accessible porosity in terms of its chemical distance λ from the exterior (Figure 4). For a sphere with $R = 1000$, 50% of accessible porosity is within $\lambda = 232$ from the exterior at $p = 1.0$; at $p = p_c$ the distance is 3.5 times greater. If we consider the farthest 10% of accessible porosity, the ratio exceeds 10 (562 versus 5840). In fact, at p_c in a sphere with $R = 1000$, there are some accessible pores at $\lambda >$ 25,000. This aspect of the accessible volume distribution will become important in understanding diffusion.

[28] It would be convenient if the distribution of accessible porosity with chemical distance from the exterior could be described as a simple function of (say) equations (4), (6), and (10). However, the distribution of accessible porosity at distances $\lambda > \chi$ is somewhat more complex (Figure 5), having a local minimum and maximum over much of the range of interest of p, and we are not aware of any analytical approximation.

4.3. Diffusion

[29] The loss of solute from a homogeneous porous sphere initially at equilibrium with the surrounding fluid was one of many diffusion scenarios analyzed by John Crank. *Crank*'s [1975, equation 6.20] analytical solution gives the mass of solute remaining in the sphere as a function of time:

$$\frac{M(t)}{M_0} = \frac{6}{\pi^2}\sum_{n=1}^{\infty}\frac{1}{n^2}\exp\left(-\mathcal{D}n^2\pi^2 t/R^2\right), \tag{12}$$

where $M(t)$ is the mass of solute still in the sphere at time t, M_0 is the mass of solute in the sphere at time $t = 0$, and $\mathcal{D}$ is the diffusion coefficient. Diffusion on a fully connected ($p = 1.0$) cubic lattice, with random walkers moving one lattice unit in one time step, has a diffusion coefficient $\mathcal{D} = 1/6$ (lattice units)^2/time step [*Ewing and Horton*, 2002]. For a given size sphere, at full connectivity ($p = 1.0$), the Crank solution (Figure 6a) and the random walk simulation results (Figure 6b) are virtually identical. Decreasing $\mathcal{D}$ by a factor of 10 simply shifts the Crank curve to the right by a factor of 10 (Figure 6a); the shape of the curve does not change. As p decreases, the random walk simulated curve also appears to shift to the right, as if the diffusion coefficient were decreasing, but closer examination shows that the curve is being stretched rather than shifted. As p approaches p_c the change in shape increases, and it is clear that the Crank solution no longer applies. This change in behavior with decreasing p is analogous to the pattern seen for ϕ_{ar} in Figure 2, and for τ in Figure 3b: Decreasing connectivity to slightly less than $p = 1.0$ mainly changes the values by a simple scalar, but close to p_c the entire distribution changes.

[30] Because the random walkers are started with equal probability from any accessible site, their initial distribution is asymptotically identical to that of the accessible porosity (Figure 2). When the connectivity is at p_c, most of the accessible porosity is close to the sphere's exterior; this accounts for the initial fractional loss of mass being faster at low than at high connectivity (Figure 6b). But also at $p = p_c$, the time required to lose 99% of the mass (almost 10^{10} time steps for $R = 500$) is similar to that needed for $p = 1.0$ and $\mathcal{D} = 1/60{,}000$ (lattice units)^2/time step (Figure 6a). In other words, at low pore connectivity, the release of solute by diffusion is "too fast" at early times (in comparison with

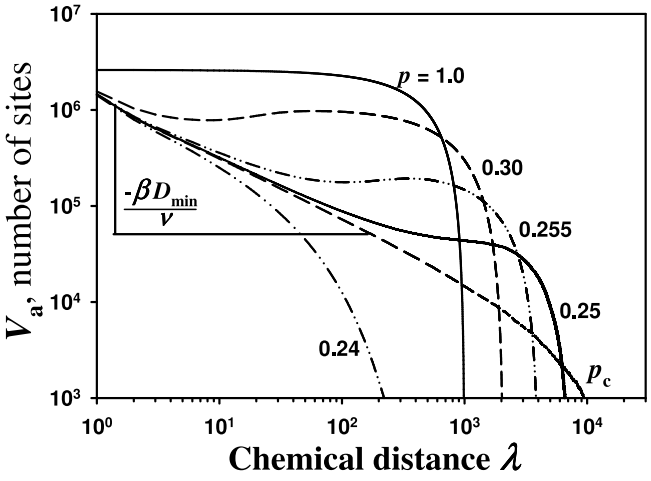

Figure 5. Accessible volume V_a as a function of chemical distance from the exterior of a sphere with $R = 1000$. The diagonal differs from that for Euclidean distance (Figure 2) by a power $D_{min} \approx 1.34$. Note the secondary maxima and minima for $p = 0.3$ and $p = 0.255$.

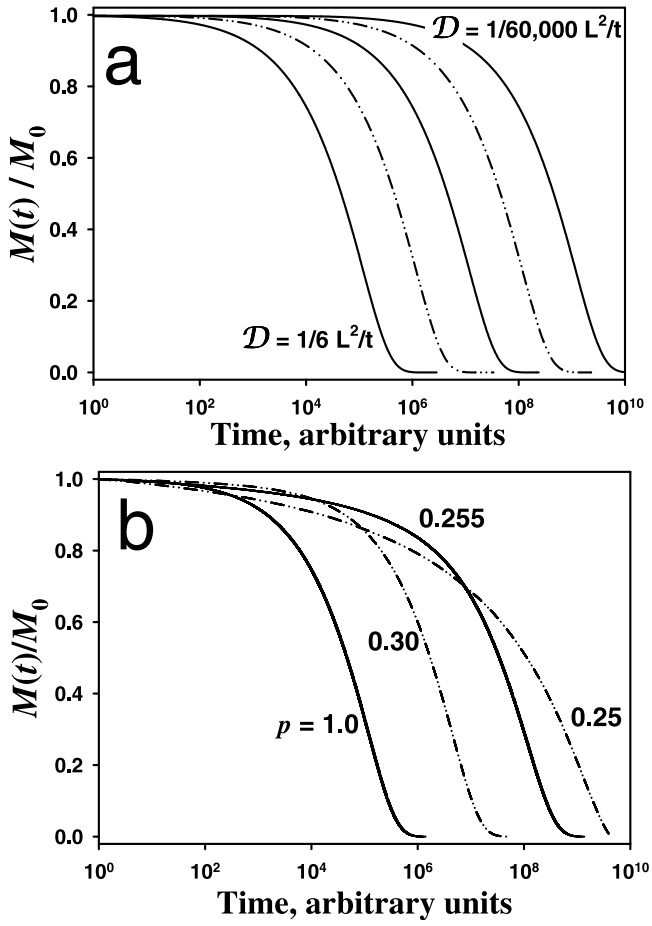

Figure 6. Mass fraction remaining ($M(t)/M_0$) as a function of time for a sphere of $R = 500$. (a) Crank's equation (equation (12) calculated for five diffusion coefficients varying by a factor of 10). (b) Four connectivities simulated via random walks.

the analytical expression, equation (12)), and "too slow" at late times. This is the same tendency frequently seen in the literature [e.g., *Werth and Hansen*, 2002], as discussed in section 1.

[31] A plot of $\log(M(t)/M_0)$ versus time produces a curve that is initially nonlinear, but asymptotically approaches a straight line. The adjustment time t_a during which the plot is nonlinear can be estimated as $t_a = R^2/(\pi^2\ \mathcal{D})$ [*Rao et al.*, 1980; *Grathwohl and Reinhard*, 1993]. Using *Crank*'s [1975] analytical solution (equation (12)), we see that only about 23% of the initial solute mass remains at t_a (Figure 7a). The apparent diffusion coefficient $\mathcal{D}_{app}$ can be obtained from this plot as

$$\mathcal{D}_{app} = -\frac{R^2}{\pi^2}\frac{\Delta \log\left(\frac{M(t)}{M_0}\right)}{\Delta t}, \qquad (13)$$

again with units of (lattice units)^2/time step. We call this coefficient "apparent" because in an experiment it is derived from measurements, the values of which depend on the time of the measurement. Whatever the "true" value of $\mathcal{D}_{app}$, if the slope ($\Delta\log(M(t)/M_0)/\Delta t$) is calculated prior to t_a, then $\mathcal{D}_{app}$ will be over-estimated. Moreover, an overestimate of $\mathcal{D}_{app}$ will underestimate the value of t_a, effectively justifying the estimated (but too early) value. If t_a is not known in advance, $\mathcal{D}_{app}$ must be calculated continuously to determine whether it has reached a constant value. Because the slope changes in logarithmic time (Figure 7b), it is easy to delude oneself that the slope is flattening long before the actual t_a.

[32] $\mathcal{D}_{app}$ was calculated from the $R = 500$ simulation results, using 20-particle neighborhoods to determine the local slope (Figure 8). With decreasing pore connectivity, the adjustment period is much longer, increasing the likelihood (in an experimental setting) of impatiently accepting a $\mathcal{D}_{app}$ value too early in the diffusion process, i.e., of overestimating $\mathcal{D}_{app}$. Additionally, near p_c, as p decreases the initial value of $\mathcal{D}_{app}$ is greater, values drop faster with time during the nonlinear period, and the early time plots have increasingly positive curvature (Figure 8). Consequently, low p increases both the likelihood of calculating $\mathcal{D}_{app}$ too early, and also the magnitude of the error incurred by doing so.

[33] When $\mathcal{D}_{app}$ is presented in terms of the mass fraction remaining (Figure 9) rather than the elapsed time (Figure 8), several additional points stand out: (1) For $p > 0.25$ the

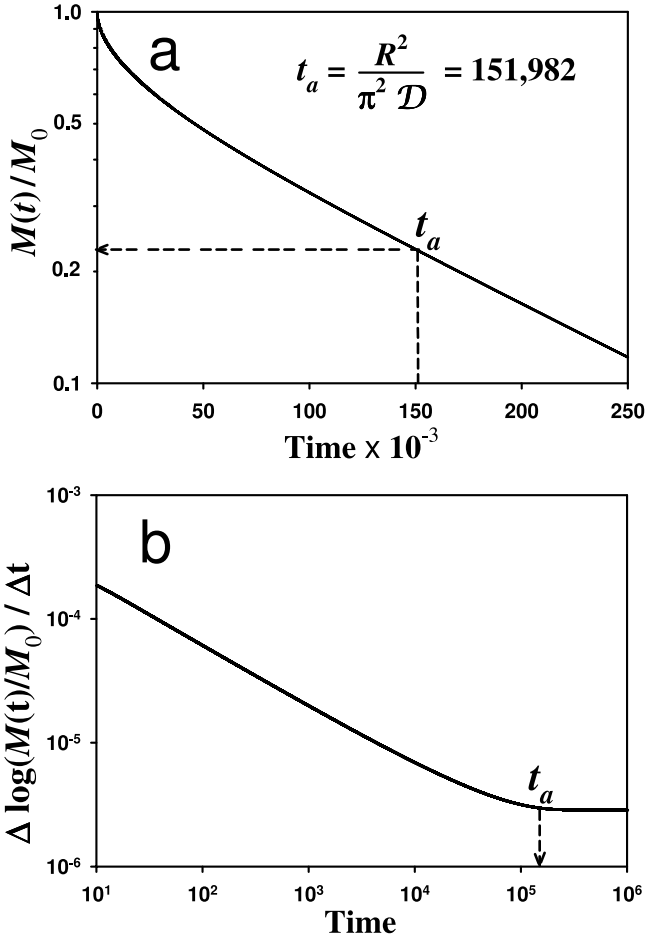

Figure 7. (a) Mass fraction remaining ($M(t)/M_0$) and (b) slope of log (mass fraction remaining) over time, both as functions of time. Numbers are from Crank's equation (equation (12)) with $R = 500$ and $\mathcal{D} = 1/6$. Note that the time axis is linear in Figure 7a and logarithmic in Figure 7b. The initial adjustment time t_a has the same value in both plots.

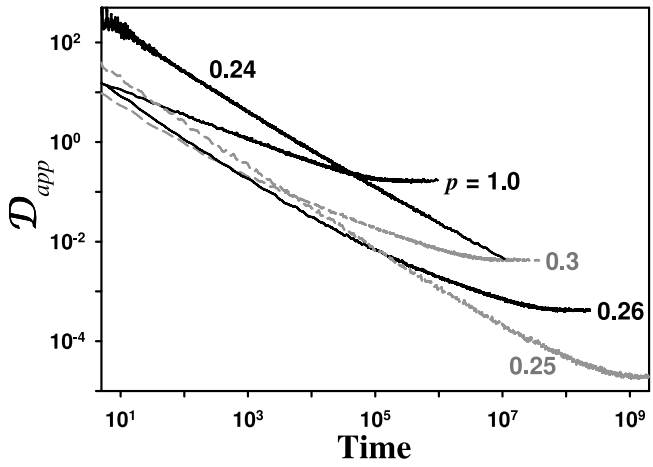

Figure 8. Apparent diffusivity $\mathcal{D}_{app}$ calculated at multiple times and for several values of the connection probability p. $\mathcal{D}_{app}$ for $p = 1.0$ reaches a final value of 1/6, the theoretical value for a simple cubic lattice.

value of $\mathcal{D}_{app}$ becomes stable when about 25% of the mass remains, consistent with *Rao et al.*'s [1980] guideline for homogeneous spheres (Figure 7); (2) at $p = 0.25$, and possibly within the range $p_c \le p \le 0.25$, the value of $\mathcal{D}_{app}$ has a local minimum rather than a simple late time stable value; (3) at $p < p_c$, $\mathcal{D}_{app}$ decreases with decreasing mass fraction remaining (or increasing time) without ever reaching a stable value; and (4) at high values of $M(t)/M_0$, $\mathcal{D}_{app}$ is greater at low values of p than at high p values (most obviously for $p = 0.24$, but evident even at $p = 0.27$). This last point, also evident in Figure 8, is counterintuitive: How can $\mathcal{D}$ be higher at low connectivity? A simple explanation can be inferred from Figure 4: At p_c, 20% of the accessible porosity is closer to the sphere's surface than is the case for $p = 1.0$. For example, at $p = p_c$, 10% of the solute mass is within $\lambda = 21$ lattice units of the surface, while at $p = 1.0$, 10% is not reached until $\lambda = 40$. So the apparently greater early time diffusivity (Figure 9) is an artifact of how the accessible porosity is distributed (Figure 4).

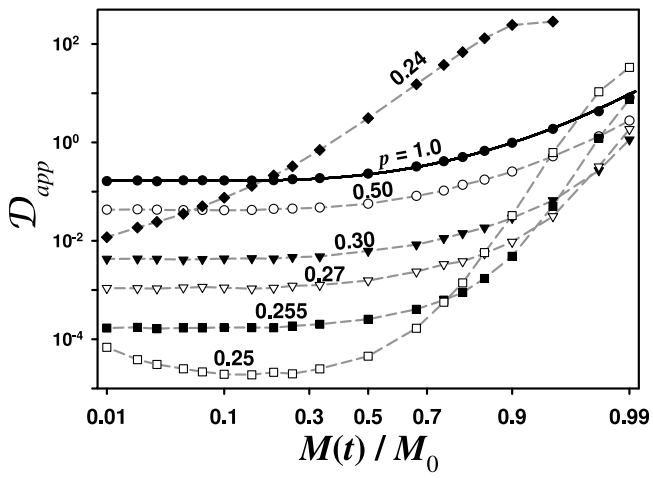

Figure 9. Apparent diffusivity $\mathcal{D}_{app}$ as a function of the mass fraction remaining ($M(t)/M_0$) for a sphere of radius $R = 500$. The solid line for $p = 1.0$ is from the *Crank* [1975] solution, equation (12); symbols are values calculated from random walk simulations. Note the probability scale of the x-axis.

[34] Solute that is initially close to the sphere's exterior, at $l < \chi$, is on finite clusters with increasing probability as $p \to p_c$. This is important, because our expectations are different for diffusion on finite clusters as opposed to the infinite cluster. Diffusion on the infinite cluster has an apparent diffusivity that scales with proximity to the percolation threshold (Figure 10) as

$$\mathcal{D}_{app} \sim (p - p_c)^{1.4}. \tag{14}$$

The values of $\mathcal{D}_{app}$ used to examine this relationship were obtained using equation (13) at $M(t)/M_0 = 10\%$ (see Figure 9). The exponent in equation (14) was historically given as $\mu - \beta$ [e.g., *Havlin and Ben Avraham*, 1987], which equaled 1.47 for the then-accepted value of the conductivity exponent, $\mu_{old} \approx 1.88$ in three dimensions. But using the currently accepted value, $\mu = 2.0$, the exponent $\mu - \beta \approx 1.59$ is not supported by our results. *Stauffer and Aharony* [1994] imply that for finite clusters, the scaling exponent in equation (14) should be $2\nu - \beta \approx 1.35$. Other considerations suggest that the exponent in equation (14), for the infinite cluster, is $(2 + \vartheta)/2D_{min} \approx 1.42$ in three dimensions; the derived exponent $\vartheta \equiv (\mu - \beta)/\nu$ (≈ 1.8 in three dimensions) appears frequently in the literature on percolation and diffusion.

[35] Regardless of the connection probability, there is a minimum value of $\mathcal{D}_{app}$ for any given sphere radius R (Figure 10), given by

$$\mathcal{D}_{app} \sim R^{-\vartheta}. \tag{15}$$

This minimum $\mathcal{D}_{app}$ is reached approximately when the radius exceeds the correlation length. When $R > \chi$, pores at a distance $l > \chi$ from the exterior are on the infinite cluster, which is statistically homogeneous. Solute that "starts" at a distance $l > \chi$ inside the sphere tends to diffuse out later than solute initially near the surface, and because it is on the infinite cluster, it behaves as if it were in a homogeneous medium with the minimum $\mathcal{D}_{app}$.

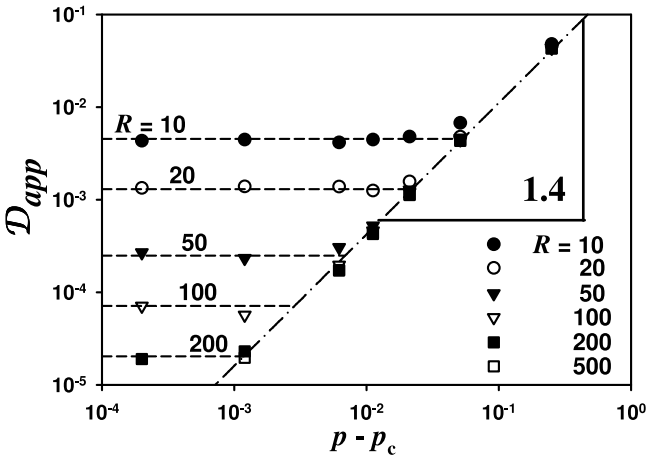

Figure 10. Predicted apparent diffusion coefficient $\mathcal{D}_{app}$ as a function of both sphere radius R and connection probability p. Symbols are simulation means; lines are from equations (14) and (15).

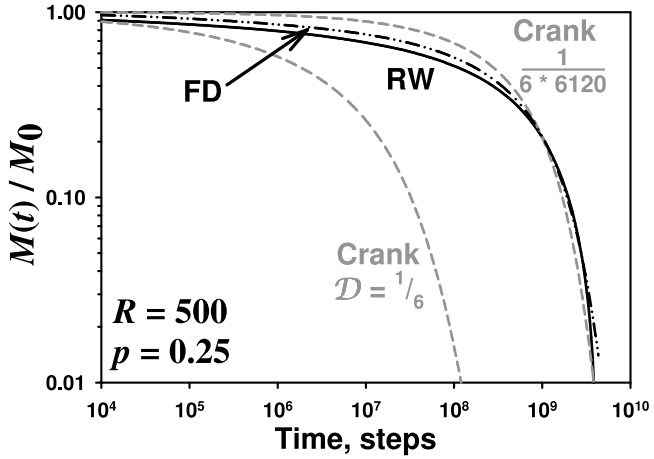

Figure 11. Mass fraction remaining with time $M(t)/M_0$, as given by random walk (RW), finite difference (FD), and Crank (equation (12)). Crank is shown at both $\mathcal{D} = 1/6$ ($p = 1.0$) and a $\mathcal{D}$ value visually adjusted to match the RW results at $M(t)/M_0 = 0.01$.

[36] As p decreases toward p_c, $\mathcal{D}_{app}$ transitions from scaling with respect to the connectivity (equation (14)) to a constant scale-dependent value (equation (15)). The intersection, at

$$R^{-\vartheta} = (p - p_c)^{(2+\vartheta)/2 \cdot D_{\min}} \tag{16a}$$

or perhaps

$$R^{-\vartheta} = (p - p_c)^{2\nu - \beta} \tag{16b}$$

identifies the crossover in diffusion behavior from a high-connectivity and/or large R regime to a low connectivity and/or small R regime. We would expect the crossover to occur at the correlation length χ, but rearranging gives the distance scaling with an exponent $-(2 + \vartheta)/2\vartheta\ D_{\min} \approx -0.786$ (equation (16a)) or $(\beta - 2\nu)/\vartheta \approx -0.75$ (equation (16b)), whereas the correlation length scaling exponent $-\nu \approx -0.88$ (equation (1)). Forcing this crossover to scale exactly with the correlation length would require the exponent in equation (14) to be $\mu - \beta \approx 1.59$, which is not supported by our results. It is not clear at this point whether this result is particular to the finite size systems we examined.

5. Discussion

[37] The picture given here of slow solute desorption from a porous sphere is considerably more complex than *Crank*'s [1975] model, and one may reasonably ask whether the improved predictions justify the additional work. In response, we note that many current models require large numbers of fitting parameters. A strength of the percolation approach explored here is that often the scaling relationships are known in advance, as are the values of their exponents. In this study, with many of the "new" parameters already known, curve fitting was never used to evaluate more than two parameters. So despite the apparent increase in complexity, there are often fewer unknowns. Additionally, the final relationships are physically based, in contrast to those often seen in ad hoc or empirical models.

[38] We have frequently cautioned that the prefactors are specific to the lattice and geometry used. Use of the word "lattice" may imply that the relationships examined here would not arise in the context of more chaotic topologies, such as might be found in intragranular pore spaces. But in fact, percolation theory can also describe irregular networks [e.g., *Jerauld et al.*, 1984a, 1984b], and in its "continuum" form [*Stauffer and Aharony*, 1994; *Hunt*, 2004] it works with, for example, random packings of interpenetrating spheres. With occasional exceptions, the universality of percolation scaling relationships means that work performed on regular lattices applies to the irregular networks found in natural porous media. This is a key point, because network models are computationally demanding and typically simulate only a small fraction of the domain of interest. The utility of this work lies not in further network modeling but in using the resulting scaling relationships in more conventional models.

[39] We examined this utility by incorporating the scaling relationships into a finite difference (FD) model, and comparing its predictions with both Crank (equation (12)) and the random walk (RW) simulation results. The cases compared used the $R = 500$ sphere with $0.25 \le p \le 1.0$. For Crank, for $p < 1.0$, the value of $\mathcal{D}$ was adjusted so as to match the RW results at $M(t)/M_0 = 1\%$. The FD model was "given" the values for R, p, $\mathcal{D}$ at $p = 1.0$, and equations (4) through (10). Using these it calculated an effective diffusivity $\mathcal{D}_{eff}$ in each layer using the common formulation [e.g., *Epstein*, 1989]

$$\mathcal{D}_{eff} = \mathcal{D}_{aq} \frac{\phi_a}{\tau^2} \tag{17}$$

with $\mathcal{D}_{aq}$ set to 1/6 lattice units/(time step)^2.

[40] While the three methods are indistinguishable at $p = 1.0$, they differ increasingly as p approaches p_c. In all cases with $p < 1.0$, the FD results had a shape between the Crank and RW results, indicating that the changes were in the right "direction" (Figure 11). If $\mathcal{D}_{eff}$ was rescaled to yield the theoretical $\mathcal{D}$ at the center (equation (15), because in all these cases $\chi < R$), the FD results shifted noticeably closer to RW. At $p = 0.25$, this rescaling further decreased $\mathcal{D}_{eff}$ by a factor of about 15. Changing the prefactor a in equation (1) (thereby changing the values of χ, b, ϕ_0, and τ_0) did not improve the match. While the agreement is not perfect, the scaling relationships appropriately changed the shape and position of the FD solute release curves, matching the RW results better than Crank did. An ongoing study examining diffusion starting from nonequilibrium will further develop the FD model.

[41] It is beyond the scope of this study to develop experimental methods to parameterize such FD models, but here we mention some possible approaches. Laser ablation can give a solute concentration profile with distance l from the surface at millimeter [e.g., *Hu and Möri*, 2008] or even micron scale [*Ewing and Horton*, 2003], which at solute equilibrium would give values for χ and ϕ_0. Parameters such as (mean) intragranular porosity and (mean) tortuosity can also be obtained by analysis of microtomographic images [e.g., *Gouze et al.*, 2008]; presumably χ and ϕ_0 could also be obtained if the images were analyzed for it. Finally, sorption/desorption studies on multiple, narrowly defined size fractions (preferably well rounded in shape)

may reveal some scale-dependent differences; the resulting data could be used to estimate values of χ, ϕ_0, and τ_0 with standard inverse methods, thereby giving $\mathcal{D}(l)$ based on the scaling relationships. Note that given those parameter values, an actual value for $p - p_c$, or $\theta - \theta_c$, is not needed.

[42] Sometimes the parameters obtained at the grain scale are precisely the parameters controlling the unexplained behavior of the system [*Gouze et al.*, 2008]. An ingenious indirect approach to obtaining pore connectivity was developed by Seaton and coworkers [*Seaton*, 1991; *Liu et al.*, 1992], based on comparing N_2 sorption/desorption isotherms generated experimentally and by pore scale network models. As seen in the present study, parameter values can change radically near the percolation threshold. But because Seaton's method is predicated on the pore connectivity being one of those values that changes so much, it is sensitive in precisely the range of interest.

[43] The phenomenon of slow sorption is sometimes considered to result from sorption nonequilibrium, with solutes progressively migrating from rapid-sorption/desorption sites to slower, stronger sorption sites. This study does not address chemical sorption as such. However, by providing a physical basis for intraparticle transport equilibrium requiring many years, it supports transport nonequilibrium as a possible explanation of slow sorption. That is, if the system is at equilibrium before desorption is initiated, the observed low porosity and high inferred tortuosity provide a reasonable explanation for extremely slow desorption. Furthermore, if desorption is initiated before solute equilibrium is attained, some solute will continue diffusing inward even while solute closer to the exterior is diffusing outward [*Borglin et al.*, 1996; *Sabbah et al.*, 2005; *Haws et al.*, 2007], further stretching the desorption curve. Note that reversible sorption/desorption with approximately linear isotherms may present as a lower apparent diffusivity [*Young and Ball*, 1994], slowing the progress toward equilibrium.

[44] The scaling relationships examined in this paper are, with minor exceptions, as would be expected on purely percolation theoretical grounds. This is gratifying, because percolation theory is usually applied to properties and processes in bulk, rather than to properties and processes as affected by an edge or within a small body. Confirming the theory's applicability to this geometry expands our toolbox of conceptual and mathematical scaling methods.

[45] Finally, we raise a potential complication. The work presented here is based on the assumption that the connection probability p is statistically stationary (spatially homogeneous). But more realistically, as a grain weathers, the pore connectivity and/or size may increase near the exterior while remaining constant deeper inside. The resulting nonuniform porosity may (1) occur in a well-connected pore network and thus have no basis in low pore connectivity, or (2) exaggerate the percolation-based distribution of accessible porosity that we examine in this work. The first possibility would be well described by the work of *Başağaoğlu et al.* [2004]. The second would result in what is known as gradient percolation [*Gouyet and Rosso*, 2005], in which there is a directional (radial in a sphere) gradient to the connection probability. This is less well studied, and presumably the scaling relationships would be changed in some way that is specific to the nature of the gradient. It is possible that some combination of this work and that of *Başağaoğlu et al.* [2004] would work in such media.

6. Conclusions

[46] We examine low pore connectivity as a possible cause of nonuniform intragranular porosity via pore-scale network modeling, and analyze the results using percolation theory. We conclude the following:

[47] 1. Low pore connectivity can produce nonuniform intragranular porosity consistent with that conjectured by *Başağaoğlu et al.* [2004].

[48] 2. Simulated solute release from a sphere with low pore connectivity deviates from the analytical solution in a manner that is consistent with observed deviations.

[49] 3. Simulated accessible porosity, diffusivity, and tortuosity are well described by the scaling equations of percolation theory.

[50] 4. Simulation results and scaling relationships indicate that the relevant parameters vary with both pore connectivity and particle radius, with the correlation length χ providing a length scale connecting the two.

[51] 5. When integrated into a conventional finite difference model, the scaling relationships provide a consistent and physically sound way to incorporate such nonuniformities into models of diffusion in granular media.

[52] **Acknowledgments.** This research was partially supported by the Environmental Remediation Science Program (ERSP), Office of Biological and Environmental Research (BER), U.S. Department of Energy (DOE). A portion of the research was performed using EMSL, a national scientific user facility sponsored by DOE-BER and located at Pacific Northwest National Laboratory (PNNL). PNNL is operated for DOE by Battelle under contract DE-AC06-76RLO 1830. Toby Ewing thanks Allen Hunt for many fruitful discussions.

References

Archie, G. E. (1942), The electrical resistivity log as an aid in determining some reservoir characteristics, *Trans. AIME*, *146*, 54–61.

Arocha, M. A., A. P. Jackman, and B. J. McCoy (1996), Adsorption kinetics of toluene on soil agglomerates: Soil as a biporous sorbent, *Environ. Sci. Technol.*, *30*, 1500–1507, doi:10.1021/es9504294.

Ball, W. P., and P. V. Roberts (1991), Long-term sorption of laogenated organic chemicals by aquifer material: 2. Intraparticle diffusion, *Environ. Sci. Technol.*, *25*, 1237–1249, doi:10.1021/es00019a003.

Başağaoğlu, H., B. J. McCoy, T. R. Ginn, F. J. Loge, and J. P. Dietrich (2002), A diffusion limited sorption kinetics model with polydispersed particles of distinct sizes and shapes, *Adv. Water Resour.*, *25*, 755–772, doi:10.1016/S0309-1708(02)00069-6.

Başağaoğlu, H., T. R. Ginn, and B. J. McCoy (2004), Radial pore diffusion with nonuniform intraparticle porosities, *J. Environ. Eng.*, *130*, 1170–1179, doi:10.1061/(ASCE)0733-9372(2004)130:10(1170).

Bear, J. (1972), *Dynamics of Fluids in Porous Media*, Dover, New York.

Borglin, S., A. Wilke, R. Jepsen, and W. Lick (1996), Parameters affecting the desorption of hydrophobic organic chemicals from suspended sediments, *Environ. Toxicol. Chem.*, *15*, 2254–2262, doi:10.1002/etc.5620151219.

Brusseau, M. L., R. E. Jessup, and P. S. C. Rao (1989), Modeling the transport of solutes influenced by multiprocess nonequilibrium, *Water Resour. Res.*, *25*, 1971–1988, doi:10.1029/WR025i009p01971.

Brusseau, M. L., R. E. Jessup, and P. S. C. Rao (1992), Modeling solute transport influenced by multiprocess nonequilibrium and transformation reactions, *Water Resour. Res.*, *28*, 175–182, doi:10.1029/91WR02497.

Cheadle, M. J., M. T. Elliott, and D. McKenzie (2004), Percolation threshold and permeability of crystallizing igneous rocks: The importance of textural equilibrium, *Geology*, *32*, 757–760, doi:10.1130/G20495.1.

Chelidze, T. L. (1982), Percolation and fracture, *Phys. Earth Planet. Inter.*, *28*, 93–101, doi:10.1016/0031-9201(82)90075-9.

Clennell, M. B. (1997), Tortuosity: A guide through the maze, in *Developments in Petrophysics*, edited by M. A. Lovell and P. K. Harvey, *Geol. Soc. Spec. Publ.*, *122*, 299–344.

Cornelissen, G., P. C. M. van Noort, and H. A. J. Govers (1997), Desorption kinetics of chlorobenzenes, polycyclic aromatic hydrocarbons, and polychlorinated biphenyls: Sediment extraction with Tenax® and effects of contact time and solute hydrophobicity, *Environ. Toxicol. Chem.*, *16*, 1351–1357, doi:10.1002/etc.5620160703.

Crank, J. (1975), *The Mathematics of Diffusion*, 2nd ed., Clarendon, Oxford, U. K.

Cunningham, J. A., and P. V. Roberts (1998), Use of temporal moments to investigate the effects of nonuniform grain-size distribution on the transport of sorbing solutes, *Water Resour. Res.*, *34*, 1415–1425, doi:10.1029/98WR00702.

Cunningham, J. A., C. J. Werth, M. Reinhard, and P. V. Roberts (1997), Effects of grain-scale mass transfer on the transport of volatile organics through sediments: 1. Model development, *Water Resour. Res.*, *33*, 2713–2726, doi:10.1029/97WR02425.

Cvetkovic, V., and H. Cheng (2008), Sorbing tracer experiments in a crystalline rock fracture at Äspö (Sweden): 3. Effect of microscale heterogeneity, *Water Resour. Res.*, *44*, W12447, doi:10.1029/2007WR006797.

Dykhuizen, R. C., and W. H. Casey (1989), An analysis of solute diffusion in rocks, *Geochim. Cosmochim. Acta*, *53*, 2797–2805, doi:10.1016/0016-7037(89)90157-9.

Eberhardt, C., and P. Grathwohl (2002), Time scales of organic contaminant dissolution from complex source zones: Coal tar pools vs. blobs, *J. Contam. Hydrol.*, *59*, 45–66, doi:10.1016/S0169-7722(02)00075-X.

Epstein, N. (1989), On tortuosity and the tortuosity factor in flow and diffusion through porous media, *Chem. Eng. Sci.*, *44*, 779–781, doi:10.1016/0009-2509(89)85053-5.

Ewing, R. P. (2009), Final report for subcontract B541028: Pore-scale modeling to support "pore connectivity" research work, *IM 370466*, Lawrence Livermore Nat'l. Lab., Livermore, Calif.

Ewing, R. P., and R. Horton (2002), Diffusion in sparsely connected pore spaces: Temporal and spatial scaling, *Water Resour. Res.*, *38*(12), 1285, doi:10.1029/2002WR001412.

Ewing, R. P., and R. Horton (2003), Diffusion scaling in low connectivity porous media, in *Scaling Methods in Soil Physics*, edited by Y. Pachepsky et al., chap. 4, pp. 49–61, CRC Press, Boca Raton, Fla.

Ewing, R. P., and A. G. Hunt (2006), Dependence of the electrical conductivity on saturation in real porous media, *Vadose Zone J.*, *5*, 731–741, doi:10.2136/vzj2005.0107.

Fleming, S. W., and R. Haggerty (2001), Modeling solute diffusion in the presence of pore-scale heterogeneity: Method development and an application to the Culebra dolomite member of the Rustler Formation, New Mexico, USA, *J. Contam. Hydrol.*, *48*, 253–276, doi:10.1016/S0169-7722(00)00182-0.

Frary, M., and C. A. Schuh (2005), Grain boundary networks: Scaling laws, preferred cluster structure, and their implications for grain boundary engineering, *Acta Mater.*, *53*, 4323–4335, doi:10.1016/j.actamat.2005.05.030.

Gouyet, J.-F., and M. Rosso (2005), Diffusion fronts and gradient percolation: A survey, *Physica A*, *357*, 86–96, doi:10.1016/j.physa.2005.05.054.

Gouze, P., Y. Melean, T. Le Borgne, M. Dentz, and J. Carrera (2008), Non-Fickian dispersion in porous media explained by heterogeneous microscale matrix diffusion, *Water Resour. Res.*, *44*, W11416, doi:10.1029/2007WR006690.

Grathwohl, P., and M. Reinhard (1993), Desorption of trichloroethylene in aquifer material: Rate limitation at the grain scale, *Environ. Sci. Technol.*, *27*, 2360–2366, doi:10.1021/es00048a008.

Gueguen, Y., T. Chelidze, and M. Le Ravalec (1997), Microstructures, percolation thresholds, and rock physical properties, *Tectonophysics*, *279*, 23–35, doi:10.1016/S0040-1951(97)00132-7.

Haggerty, R., and S. M. Gorelick (1995), Multiple-rate mass transfer for modeling diffusion and surface reactions in media with pore-scale heterogeneity, *Water Resour. Res.*, *31*, 2383–2400, doi:10.1029/95WR10583.

Haggerty, R., and S. M. Gorelick (1998), Modeling mass transfer processes in soil columns with pore-scale heterogeneity, *Soil Sci. Soc. Am. J.*, *62*, 62–74.

Harmon, T. C., and P. V. Roberts (1994), Comparison of intraparticle sorption and desorption rates for a halogenated alkene in a sandy aquifer material, *Environ. Sci. Technol.*, *28*, 1650–1660, doi:10.1021/es00058a017.

Hatzinger, P. B., and M. Alexander (1995), Effect of aging of chemicals in soil on their biodegradability and extractability, *Environ. Sci. Technol.*, *29*, 537–545, doi:10.1021/es00002a033.

Havlin, S., and D. Ben-Avraham (1987), Diffusion in disordered media, *Adv. Phys.*, *36*, 695–798, doi:10.1080/00018738700101072.

Haws, N. W., W. P. Ball, and E. J. Bouwer (2007), Effects of initial solute distribution on contaminant availability, desorption modeling, and subsurface remediation, *J. Environ. Qual.*, *36*, 1392–1402, doi:10.2134/jeq2006.0470.

Heyse, E. C., D. J. Mika, T. P. de Venoge, D. L. Coulliette, and A. McGowin (1999), General radial diffusion model for heterogeneous sorbents, *Environ. Toxicol. Chem.*, *18*, 1694–1700, doi:10.1002/etc.5620180813.

Ho, Y. S., J. C. Y. Ng, and G. McKay (2000), Kinetics of pollutant sorption by biosorbents, Review, *Separ. Purif. Methods*, *29*, 189–232, doi:10.1081/SPM-100100009.

Hu, Q. H., and R. P. Ewing (2002), Pore connectivity effects on solute transport in rocks, in *Bridging the Gap Between Measurements and Modelling in Heterogeneous Media: Proceedings of the International Groundwater Symposium*, edited by A. N. Findikakis, pp. 583–587, Int. Assoc. for Hydro-Environ. Eng. and Res., Madrid.

Hu, Q. H., and A. Möri (2008), Radionuclide transport in fractured granite interface zones, *Phys. Chem. Earth*, *33*, 1042–1049, doi:10.1016/j.pce.2008.05.015.

Hu, Q. H., R. P. Ewing, L. Tomutsa, and M. J. Singleton (2006), Pore connectivity, episodic flow, and unsaturated diffusion in fractured tuff, in *Proceedings of the 11th International High-Level Radioactive Waste Management Conference (IHLRWM)*, pp. 70–76, Am. Nucl. Soc., La Grange Park, Ill.

Hunt, A. G. (2004), Continuum percolation theory and Archie's law, *Geophys. Res. Lett.*, *31*, L19503, doi:10.1029/2004GL020817.

Hunt, A. G. (2005), Basic transport properties in natural porous media, *Complexity*, *10*, 22–37, doi:10.1002/cplx.20067.

Hunt, A. G., and R. P. Ewing (2009), *Percolation Theory for Flow in Porous Media*, 2nd ed., *Lect. Not. Phys.*, 771, Springer, Berlin.

Jerauld, G. R., J. C. Hatfield, L. E. Scriven, and H. T. Davis (1984a), Percolation and conduction on Voronoi and triangular networks: A case study in topological disorder, *J. Phys. C*, *17*, 1519–1529, doi:10.1088/0022-3719/17/9/010.

Jerauld, G. R., L. E. Scriven, and H. T. Davis (1984b), Percolation and conduction on the 3D Voronoi and regular networks: A second case study in topological disorder, *J. Phys. C*, *17*, 3429–3439, doi:10.1088/0022-3719/17/19/017.

Karmakar, R., S. S. Manna, and T. Dutta (2003), A geometrical model of diagenesis using percolation theory, *Physica A*, *318*, 113–120, doi:10.1016/S0378-4371(02)01413-9.

Kleineidam, S., H. Rügner, and P. Grathwohl (1999), Impact of grain scale heterogeneity on slow sorption kinetics, *Environ. Toxicol. Chem.*, *18*, 1673–1678, doi:10.1002/etc.5620180810.

Ko, D. C. K., D. H. K. Tsang, J. F. Porter, and G. McKay (2003), Applications of multipore model for the mechanism identification during the adsorption of dye on activated charcoal and bagasse pith, *Langmuir*, *19*, 722–730, doi:10.1021/la020654g.

Li, J., and C. J. Werth (2004), Slow desorption mechanisms of volatile organic chemical mixtures in soil and sediment micropores, *Environ. Sci. Technol.*, *38*, 440–448, doi:10.1021/es034830z.

Liedl, R., and T. Ptak (2003), Modelling of diffusion-limited retardation of contaminants in hydraulically and lithologically nonuniform media, *J. Contam. Hydrol.*, *66*, 239–259, doi:10.1016/S0169-7722(03)00028-7.

Liu, H., L. Zhang, and N. A. Seaton (1992), Determination of the connectivity of porous solids from nitrogen sorption measurements: II. Generalisation, *Chem. Eng. Sci.*, *47*, 4393–4404, doi:10.1016/0009-2509(92)85117-T.

Matsumoto, M., and T. Nishimura (1998), Mersenne Twister: A 623-dimensionally equidistributed uniform pseudo-random number generator, *ACM Trans. Model. Comput. Simul.*, *8*, 3–30, doi:10.1145/272991.272995.

Moldrup, P., T. Olesen, T. Komatsu, P. Schjønning, and D. E. Rolston (2001), Tortuosity, diffusivity, and permeability in the soil liquid and gaseous phases, *Soil Sci. Soc. Am. J.*, *65*, 613–623.

Nestle, N. F. E. I., and R. Kimmich (1996), Concentration-dependent diffusion coefficients and sorption isotherms: Application to ion exchange processes as an example, *J. Phys. Chem.*, *100*, 12,569–12,573, doi:10.1021/jp960342k.

Niedermeier, C. A., and R. C. Loehr (2005), Application of an intraparticle diffusion model to describe the release of polyaromatic hydrocarbons from field soils, *J. Environ. Eng.*, *131*, 943–951, doi:10.1061/(ASCE)0733-9372(2005)131:6(943).

Nkedi-Kizza, P., J. W. Biggar, H. M. Selim, M. T. van Genuchten, P. J. Weirenga, J. M. Davidson, and D. R. Nielsen (1985), On the equivalence of two conceptual models for describing ion exchange during transport through an aggregated oxisol, *Water Resour. Res.*, *20*, 1123–1130, doi:10.1029/WR020i008p01123.

Pedit, J. A., and C. T. Miller (1994), Heterogeneous sorption processes in subsurface systems: 1. Model formulations and applications, *Environ. Sci. Technol.*, *28*, 2094–2104, doi:10.1021/es00061a018.

Philip, J. R. (1957), The theory of infiltration: 4. Sorptivity and algebraic infiltration equations, *Soil Sci.*, *84*, 257–264.

Pignatello, J. J., and B. Xing (1996), Mechanisms of slow sorption of organic chemicals to natural particles, *Environ. Sci. Technol.*, *30*, 1–11, doi:10.1021/es940683g.

Price, J. D., D. A. Wark, E. B. Watson, and A. M. Smith (2006), Grain-scale permeabilities of faceted polycrystalline aggregates, *Geofluids*, *6*, 302–318, doi:10.1111/j.1468-8123.2006.00149.x.

Rao, P. S. C., R. E. Jessup, D. E. Rolston, J. M. Davidson, and D. P. Kilcrease (1980), Experimental and mathematical description of nonadsorbed solute transfer by diffusion in spherical aggregates, *Soil Sci. Soc. Am. J.*, *44*, 684–688.

Sabbah, I., W. P. Ball, D. F. Young, and E. J. Bouwer (2005), Misinterpretations in the modeling of contaminant desorption from environmental solids when equilibrium conditions are not fully understood, *Environ. Eng. Sci.*, *22*, 350–366, doi:10.1089/ees.2005.22.350.

Scheidegger, A. E. (1960), *The Physics of Flow Through Porous Media*, 2nd ed., Univ. of Toronto Press, Toronto, Ont., Canada.

Scott, D. C. (2001), An assessment of reasonable tortuosity values, *Pharm. Res.*, *18*, 1797–1800, doi:10.1023/A:1013399302958.

Seaton, N. A. (1991), Determination of the connectivity of porous solids from nitrogen sorption measurements, *Chem. Eng. Sci.*, *46*(8), 1895–1909, doi:10.1016/0009-2509(91)80151-N.

Stauffer, D., and A. Aharony (1994), *Introduction to Percolation Theory*, 2nd ed., Taylor and Francis, London.

Steinberg, S. M., J. J. Pignatello, and B. L. Sawhney (1987), Persistence of 1,2-dibromomethane in soils: Entrapment in intraparticle micropores, *Environ. Sci. Technol.*, *21*, 1201–1208, doi:10.1021/es00165a007.

Ten Hulscher, T. E. M., B. A. Vrind, H. van den Heuvel, P. C. M. van Noort, and H. A. J. Govers (2005), Influence of long contact times on sediment sorption kinetics of spiked chlorinated compounds, *Environ. Toxicol. Chem.*, *24*, 2154–2159, doi:10.1897/04-260R.1.

Valocchi, A. J. (1985), Validity of the local equilibrium assumption for modeling sorbing solute transport through homogeneous soils, *Water Resour. Res.*, *21*, 808–820, doi:10.1029/WR021i006p00808.

Weber, W. J., Jr., W. Huang, and H. Yu (1998), Hysteresis in the sorption and desorption of hydrophobic organic contaminants by soils and sediments: 2. Effects of soil organic matter heterogeneity, *J. Contam. Hydrol.*, *31*, 149–165, doi:10.1016/S0169-7722(97)00059-4.

Werth, C. J., and K. M. Hansen (2002), Modeling the effects of concentration history on the slow desorption of trichloroethene from a soil at 100% relative humidity, *J. Contam. Hydrol.*, *54*, 307–327, doi:10.1016/S0169-7722(01)00183-8.

Werth, C. J., and M. Reinhard (1997), Effects of temperature on trichloroethylene desorption from silica gel and natural sediments: 2. Kinetics, *Environ. Sci. Technol.*, *31*, 697–703, doi:10.1021/es960231z.

Wood, W. W., T. F. Kraemer, and P. P. Hearn Jr. (1990), Intragranular diffusion: An important mechanism influencing solute transport in clastic aquifers?, *Science*, *247*, 1569–1572, doi:10.1126/science.247.4950.1569.

Wu, S.-C., and P. M. Gschwend (1986), Sorption kinetics of hydrophobic organic compounds to natural sediments and soils, *Environ. Sci. Technol.*, *20*, 717–725, doi:10.1021/es00149a011.

Xing, B., and J. J. Pignatello (1997), Dual-mode sorption of low-polarity compounds in glassy poly(vinyl chloride) and soil organic matter, *Environ. Sci. Technol.*, *31*, 792–799, doi:10.1021/es960481f.

Xu, S., and A. Wörman (1999), Implications of sorption kinetics to radionuclide migration in fractured rock, *Water Resour. Res.*, *35*(11), 3429–3440, doi:10.1029/1999WR900213.

Young, D. F., and W. P. Ball (1994), A priori simulation of tetrachloroethene transport through aquifer material using an intraparticle diffusion model, *Environ. Prog.*, *13*, 9–20, doi:10.1002/ep.670130112.

Young, D. F., and W. P. Ball (1999), Two-region linear/nonlinear sorption modeling: Batch and column experiments, *Environ. Toxicol. Chem.*, *18*, 1686–1693, doi:10.1002/etc.5620180812.

Zhu, W., and G. Hirth (2003), A network model for permeability in partially molten rocks, *Earth Planet. Sci. Lett.*, *212*, 407–416, doi:10.1016/S0012-821X(03)00264-4.

R. P. Ewing, Department of Agronomy, Iowa State University, Ames, IA 50011-1010, USA. (ewing@iastate.edu)

Q. Hu, Department of Earth and Environmental Sciences, University of Texas at Arlington, 500 Yates St., Arlington, TX 76019-0049, USA.

C. Liu, Chemical and Material Science Division, Fundamental and Computational Science Directorate, Pacific Northwest National Laboratory, Richland, WA 99354, USA.